## GEOLOGY

# Tectonic trigger to the first major extinction of the Phanerozoic: The early Cambrian Sinsk event

Paul M. Myrow[1]*, John W. Goodge[2,3], Glenn A. Brock[4], Marissa J. Betts[5], Tae-Yoon S. Park[6,7], Nigel C. Hughes[8], Robert R. Gaines[9]

The Cambrian explosion, one of the most consequential biological revolutions in Earth history, occurred in two phases separated by the Sinsk event, the first major extinction of the Phanerozoic. Trilobite fossil data show that Series 2 strata in the Ross Orogen, Antarctica, and Delamerian Orogen, Australia, record nearly identical and synchronous tectono-sedimentary shifts marking the Sinsk event. These resulted from an abrupt pulse of contractional supracrustal deformation on both continents during the *Pararaia janeae* trilobite Zone. The Sinsk event extinction was triggered by initial Ross/Delamerian supracrustal contraction along the edge of Gondwana, which caused a cascading series of geodynamic, paleoenvironmental, and biotic changes, including (i) loss of shallow marine carbonate habitats along the Gondwanan margin; (ii) tectonic transformation to extensional tectonics within the Gondwanan interior; (iii) extrusion of the Kalkarindji large igneous province; (iv) release of large volumes of volcanic gasses; and (v) rapid climatic change, including incursions of marine anoxic waters and collapse of shallow marine ecosystems.

## INTRODUCTION

The Cambrian explosion, which records the rapid radiation of most animal phyla, took place in two phases, separated by the first major extinction of the Phanerozoic, the early Stage 4 Sinsk event (1–3). This event included extinction or near extinction of many characteristic early Cambrian clades such as archaeocyathids and hyoliths, and a subsequent radiation of less affected brachiopods and trilobites, as well as changes in body sizes in various groups (4). The global increase in the abundance of unbioturbated black shale and a shift from coupled to uncoupled carbon and sulfur isotopic records all indicate that a decline in global oceanic oxygen levels played a major role in the extinction (1–3). However, the causes of these environmental and biotic changes remain poorly understood.

The Sinsk event followed a long phase of Neoproterozoic to early Paleozoic global tectonic reorganization, including breakup of the supercontinent Rodinia and reassembly of most cratonic masses into Gondwana (5). Collisional suturing during the East African and Kuunga orogenies culminated in amalgamation of East Gondwana (modern Africa, Antarctica, Australia, and India) during the Cambrian (6). Gondwana supercontinent assembly included suturing along the East African–Antarctic Orogen, broadly fusing East (Indo-Antarctica) and West (Africa) Gondwana between ~600 and 540 Ma (7–10). This, in turn, triggered geodynamic reorganization of the peri-Gondwanan realm, including a shift to widespread development of nascent convergent plate margins (10–12) and continental-margin arc magmatism that drove climatic warming that was conducive to evolutionary diversification (13, 14).

In Antarctica, this global tectonic reorganization primarily included the transition from a passive margin to an Andean-type convergent plate margin along the proto-Pacific edge of the East Antarctic craton. There, onset of subduction by ~590 million years ago (Ma) led to the Ross Orogeny, a protracted cycle of latest Neoproterozoic to Ordovician magmatism, metamorphism, deformation, and syn-tectonic erosion and sedimentation that culminated between ~525 and 490 Ma (Fig. 1) (15). The Cambrian Ross orogenic activity is well-documented in the central Transantarctic Mountains (16–18). The Delamerian Orogen in South Australia, situated along strike to the north on the Rodinian and Gondwanan margins, shows a similar tectonic history, including well-dated igneous and metamorphic events from ~515 to 490 Ma (19–21).

Here, we present data from trilobites that constrain the timing and nature of Ross Orogenic supracrustal deformation and its erosional and depositional response. These are compared with faunal data from an age-equivalent record from Kangaroo Island, South Australia, to reveal remarkable similarities in the sedimentary signal and a near-synchronous, Cambrian mid–Series 2 timing of supracrustal events in these two orogens, despite differences in paleogeographic position, timing of the onset of subduction-related magmatism, and structural styles (foreland versus forearc deformation).

These supracrustal plate-margin events were synchronous within geochronologic and biostratigraphic constraints, with a corresponding transition from compressional to extensional tectonics within the interior of post-assembly Gondwana, suggesting a causal linkage. Coupled drowning of shale basins along active plate margins and loading of the atmosphere with $CO_2$ by voluminous mantle upwelling in the extending cratonic interior together likely led to ocean warming (14), sluggish oceanic turnover, and bottom water anoxia. Critically, the timing of these changes coincides with the first major extinction of the Phanerozoic, the early Cambrian Sinsk event, a biotic crisis that included a major extinction that decimated archaeocyathids. This suggests that tectonics were acting with, and perhaps a major driver of, the widespread paleoenvironmental effects of the Sinsk event, including perturbations to the oceans, atmosphere, and biosphere.

[1]Department of Geology, Colorado College, Colorado Springs, CO 80903, USA. [2]Department of Earth and Environmental Sciences, University of Minnesota, Duluth, MN 55812, USA. [3]Planetary Science Institute, Tucson, AZ 85719, USA. [4]School of Natural Sciences, Macquarie University, North Ryde, Sydney, NSW 2109, Australia. [5]Palaeoscience Research Centre, School of Environmental and Rural Science, University of New England, Armidale, NSW 2351, Australia. [6]Division of Earth Sciences, Korea Polar Research Institute, Incheon 21990, Republic of Korea. [7]Polar Science, University of Science and Technology, Daejeon 34113, Republic of Korea. [8]Department of Earth and Planetary Sciences, University of California, Riverside, CA 92521, USA. [9]Geology Department, Pomona College, Claremont, CA 91711, USA.
*Corresponding author. Email: pmyrow@coloradocollege.edu, m_hu@coloradocollege.edu
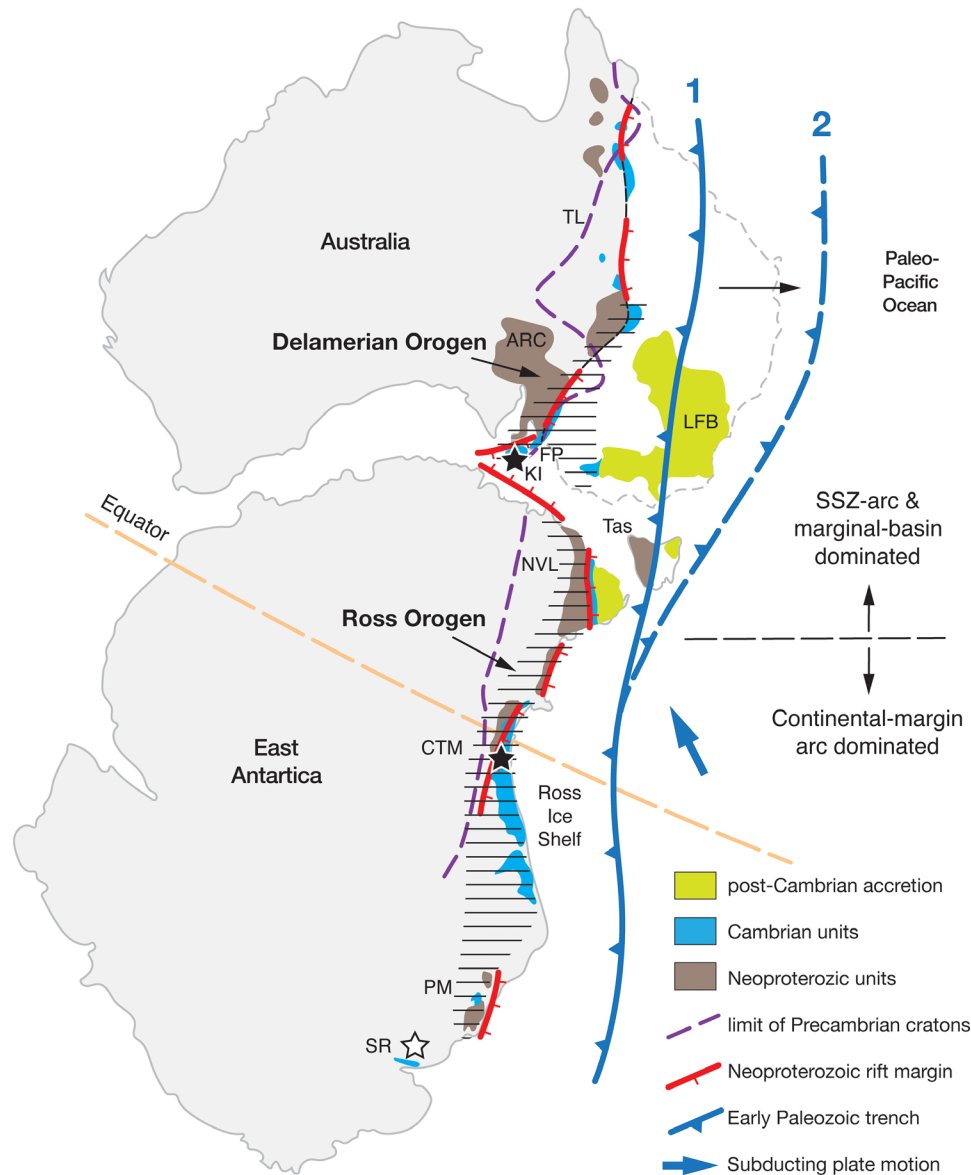
**Fig. 1. Tectonic setting of the Neoproterozoic and Cambrian systems in East Antarctica and Australia.** Locations of Kangaroo Island (KI) and Nimrod Glacier area of the central Transantarctic Mountains (CTM) shown with black stars; similar geologic relations occur in the Shackleton Range (SR), shown by a white star. Early Paleozoic trench migrated oceanward between Cambrian (1, solid line) and Devonian time (2, dashed line). ARC, Adelaide Rift Complex; FP, Fleurieu Peninsula; LFB, Lachlan Fold Belt; NVL, northern Victoria Land; PM, Pensacola Mountains; Tas, Tasmania. Reconstruction modeled from GPlates (*88*) and alignment of geophysical anomalies (*89*), with mid-Cambrian equator from Scotese (*90*). Inferred eastern edge of Precambrian cratons (purple dashed line) from Goodge and Finn (*91*) in Antarctica and Tasman Line (TL) in Australia. Distribution of sedimentary units after Foden *et al*. (*19*), Goodge (*15*), and Cox *et al*. (*92*). Extent of Ross and Delamerian orogens shown by horizontal ruling (*15*, *93*). Inferred Neoproterozoic rift-margin faults from Preiss (*30*) and Goodge (*15*). West-dipping early Paleozoic marginal subduction zone (blue barbed line) was sinistral-oblique in middle Cambrian time [line 1; (*60*)]; by late Cambrian, convergence was geometrically more complicated (line 2), including multiple arcs and back-arcs [see (*10*) and (*94*)]. Dashed line separates two convergent margin domains—to the south in East Antarctica dominated by Andean-type continental-margin magmatic arc, and to the north from northern Victoria Land into Australia dominated by accretionary supra-subduction zone volcanism and marginal-basin development.

## RESULTS

The Ross Orogen, central Transantarctic Mountains (Fig. 1), records the transition from Neoproterozoic passive-margin to Cambrian active-margin tectonics along the Austral-Antarctic periphery of Gondwana. There, Archean and Proterozoic crystalline basement is overlain by the Neoproterozoic Beardmore Group, a rift-margin succession of sandstone, shale, carbonate, diamictite, and minor volcanic rocks (*15*, *18*, *22*).

The Beardmore Group is succeeded by the lowermost Paleozoic Byrd Group, consisting of carbonate platform deposits and overlying syn-tectonic clastic molasse. The lower Cambrian Shackleton Limestone at the base is a thick carbonate unit with archaeocyathid–calcimicrobial reefs (*16*, *23*, *24*). The top of the formation is marked by intact reefs up to 38 m thick that are draped by a phosphatic hardground interpreted as a sediment starvation surface produced by rapid deepening and terminal drowning of the reef system (Fig. 2)

(16). The hardground is overlain by the Holyoake Formation, a 5- to 10-m-thick unit of dark shale and nodular carbonate that grades upward into siltstone to pebbly sandstone of the Starshot Formation, the latter comprising inner shelf to shoreline deposits. Both the Holyoake and Starshot formations locally onlap uppermost Shackleton reefs [see figure 10 of (16)].

The Starshot Formation grades upward into the Douglas Conglomerate, a thick and coarse sedimentary wedge that is laterally equivalent to (and locally both underlain and overlain by) sandstone of the Starshot. The Douglas contains fluvial and alluvial fan cobble to boulder conglomerate, sandstone, and minor shale (16). Conglomeratic channels of the Douglas cut down into reefs of the upper
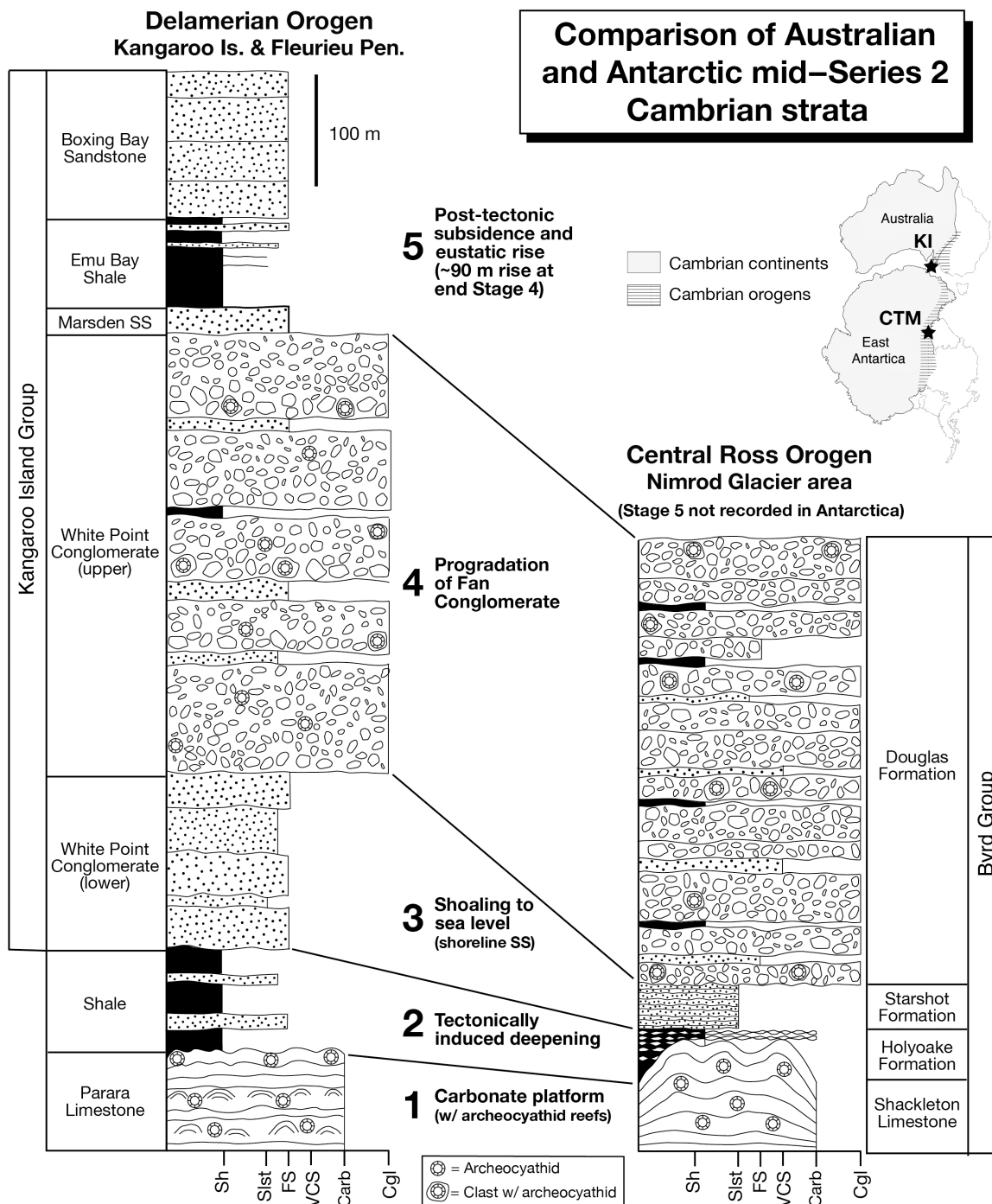


**Fig. 2. Stratigraphic comparison of Cambrian Series 2, Stage 4 strata on Kangaroo Island and central Transantarctic Mountains.** Inset shows location of sections in the restored continents (Fig. 1) and in Delamerian and Ross orogens. Stratigraphic units described in Results. The sections record five stages, from platform buildup through tectonic response to post-tectonic subsidence, although relative thicknesses and lithotypes vary. SS, sandstone; Sh, shale; Slst, siltstone; FS, fine sandstone; Carb, carbonate; Cgl, conglomerate.

Shackleton, and their fills contain archaeocyathid-bearing limestone boulders up to 2 m across (*16, 23, 24*). Overall, the succession indicates reef drowning followed by shoaling from deeper water mud through shoreline sand to subaerial coarse-grained fluvial and alluvial fan deposits.

Age constraints on the Byrd Group come from trilobites (*25*), archaeocyathids (*26*), and other fossils (*27–29*). Trilobite (*25*) and brachiopod (*28*) assemblages and a positive carbon isotopic excursion at the base (*16*) suggest that the Shackleton Formation is Cambrian Series 2, Stage 3 to lowermost Stage 4 (Atdabanian to lowermost Botoman equivalent) in age. Myrow et al. (*16*) assigned the overlying Holyoake and Starshot formations to Stage 4, or late(?) Tsanglangpuian/Botoman, based on preliminary trilobite data. We herein report trilobite data from our subsequent work (field collection in 2011) to provide a more refined age for these units. Trilobites from these units include *Meniscuchus* cf. *M. menetus*, *Pagetides* (*Discomesites*) sp., and *Hsuaspis* cf. *H. bilobata* (= *Estaingia bilobata*) (Fig. 3), the latter occurring as part of a diverse assemblage in the *Pararaia janeae* Zone near the base of Stage 4. Thus, these data constrain the timing of the abrupt switch from platform carbonate deposition to supracrustal deformation processes during Stage 4.

The Delamerian Orogeny resulted in deformation of a thick Neoproterozoic to early Cambrian rift-margin succession in South Australia (*20, 30*). The Cambrian strata include carbonate of the Kulpara and Parara formations (*31*), succeeded by fine-grained siliciclastic deposits, an unnamed shale unit in the eastern part of its outcrop area and the Mt. McDonnell Formation in the western part (Fig. 2) (*31–33*). These strata are overlain by the Kangaroo Island Group, an alluvial fan to shallow marine Cambrian succession that crops out in a small area on the northeastern coast of Kangaroo Island, southwest of the Fleurieu Peninsula (Fig. 1). It is approximately equivalent in age to the Kanmantoo Group, a metamorphosed deep-water succession that extends from Kangaroo Island northward to the eastern side of the Fleurieu Peninsula (*34, 35*). Previous workers interpreted the Kangaroo Island Group as alluvial fan to shallow marine deposits on the northern margin of an active rift basin (*34, 36–39*), tectonically linked to the Stansbury Basin (*40*).

Basal units of the Kangaroo Island Group are the White Point Conglomerate and coeval Stokes Bay Sandstone (*41*). The White Point is up to 580-m thick and contains a lower member of sandstone with minor siltstone and shale (*31, 32, 36*) and an upper conglomerate member with clasts up to 1.5 m across (*31*). The angular to subrounded clasts of the conglomerate are polymictic with basement and sedimentary cover lithologies represented (*32, 37*). Abundant carbonate clasts contain Cambrian archaeocyathids and small shelly fossils belonging to the *P. janeae* trilobite Zone, which sets a lowermost Stage 4 maximum depositional age for the unit (*34*). Pinch-out of the conglomerate to the south (*31, 41*) and clast imbrication (*32*) suggest southward fan delta progradation with a source to the north. Clasts in the White Point were likely derived from the underlying Koolywurtie Limestone Member of the Parara Limestone, which is intersected in numerous drill cores and exposed as outcrop 100 km to the north on Yorke Peninsula (*35, 42*).

Overlying deposits consist of the Marsden Sandstone, an unconformity-bound shoaling succession with a lower mudstone member, followed by mudstone and sandstone of the Emu Bay Shale, and sandstone of the Boxing Bay Formation (Fig. 2). Together, these units record pulses of marine transgression following deposition of the White Point Conglomerate (*31*). *P. janeae* Zone trilobites from the basal Marsden and from the Emu Bay indicate a Stage 4 age for these marine strata (*43*). Thus, strata from the Koolywurtie Limestone through the Emu Bay Shale all date to the *P. janeae* Zone, including the White Point Conglomerate, indicating a nearly identical timing of supracrustal deformation in this part of Australia with the central Transantarctic Mountains deformation, which we discuss below.

## DISCUSSION
Strata from the central Ross and Delamerian orogens indicate notable similarities. Both sections record: (i) drowning of a carbonate
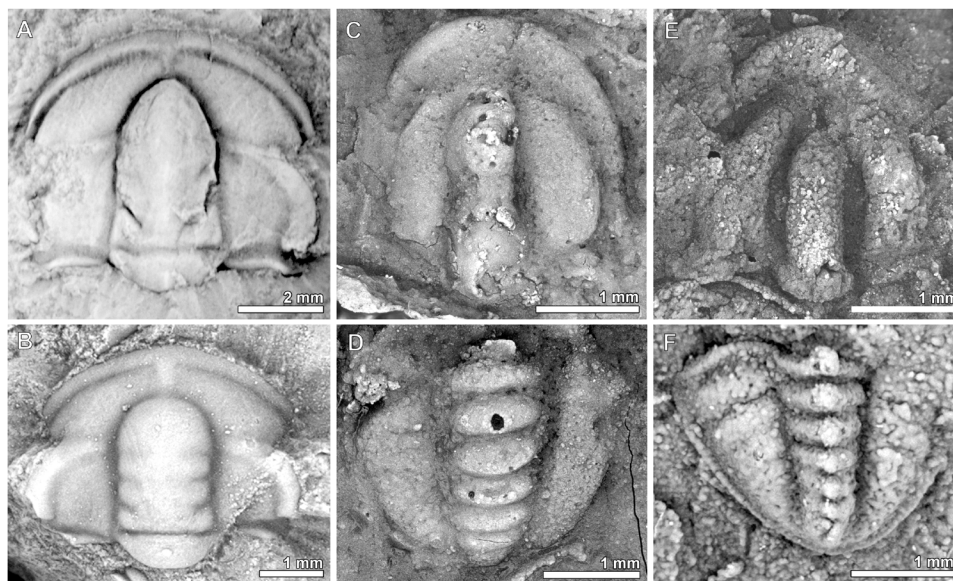


**Fig. 3. Trilobites recovered from the Holyoake Formation (82°13.185′S, 160°16.122′E).** (**A** and **B**) *Estaingia bilobata*; CMCIP 88140 and CMCIP 88142, respectively. (**C** and **D**) *Meniscuchus* cf. *M. menetus*; CMCIP 88138 and CMCIP 96988, respectively. (**E** and **F**) *Pagetides* (*Discomesites*) sp.; CMCIP 88139 and CMCIP 96989, respectively.

platform containing archaeocyathid-bearing reefs, (ii) an overlying shoaling succession of mud to sand, and (iii) continued shoaling to coarse gravel alluvial fan deposits with carbonate clasts. In Antarctica, the clastic succession represents tectonically induced subsidence associated with a major phase of supracrustal deformation during the Ross Orogeny (*16*). The timing of this deformational and erosional event is here refined to the *P. janeae* Zone of basal Cambrian Stage 4. A nearly identical sedimentary record of deformation onset, tectonic uplift, erosion, and conglomeratic deposition in South Australia also took place in the *P. janeae* Zone, as described above. Further evidence linking the geologic histories of these areas is provided by dated igneous and metamorphic events (Fig. 4). Punctuated magmatic-arc intrusive activity in both areas extended from at least 550 to 490 Ma (*17, 19, 21, 44*), indicating active plate convergence through this period. Metasedimentary $^{40}$Ar/$^{39}$Ar mineral and slate cooling ages range from ~512 to 476 Ma (Fig. 4) and record progressive cooling in

response to uplift and erosion within the deeper orogen (*17, 20, 45*). This activity corresponds closely in time with the surficial response to deformation and uplift. Thus, the depositional, igneous, and metamorphic events recorded in the central Ross and southern Delamerian orogens provide evidence for remarkable synchroneity in a late early-Cambrian tectonic pulse during long-lived plate convergence.

The base of the as-yet-undefined Cambrian Stage 4, and the *P. janeae* Zone, is known to be younger than 514.45 ± 0.36 Ma (*46*). The pulse of contractional deformation, uplift, and erosion along the Austral-Antarctic margin of Gondwana described here clearly took place within the lower part of the *P. janeae* Zone. A radiometric age of 511.87 ± 0.14 Ma (*47*) from a volcanic tuff in the Billy Creek Formation of the Flinders Range dates the middle to upper *P. janeae* Zone. The Billy Creek is correlated with trilobites to the Marsden Sandstone and Emu Bay Shale on Kangaroo Island, which rests above the syntectonic White Point Conglomerate. These relationships indicate that
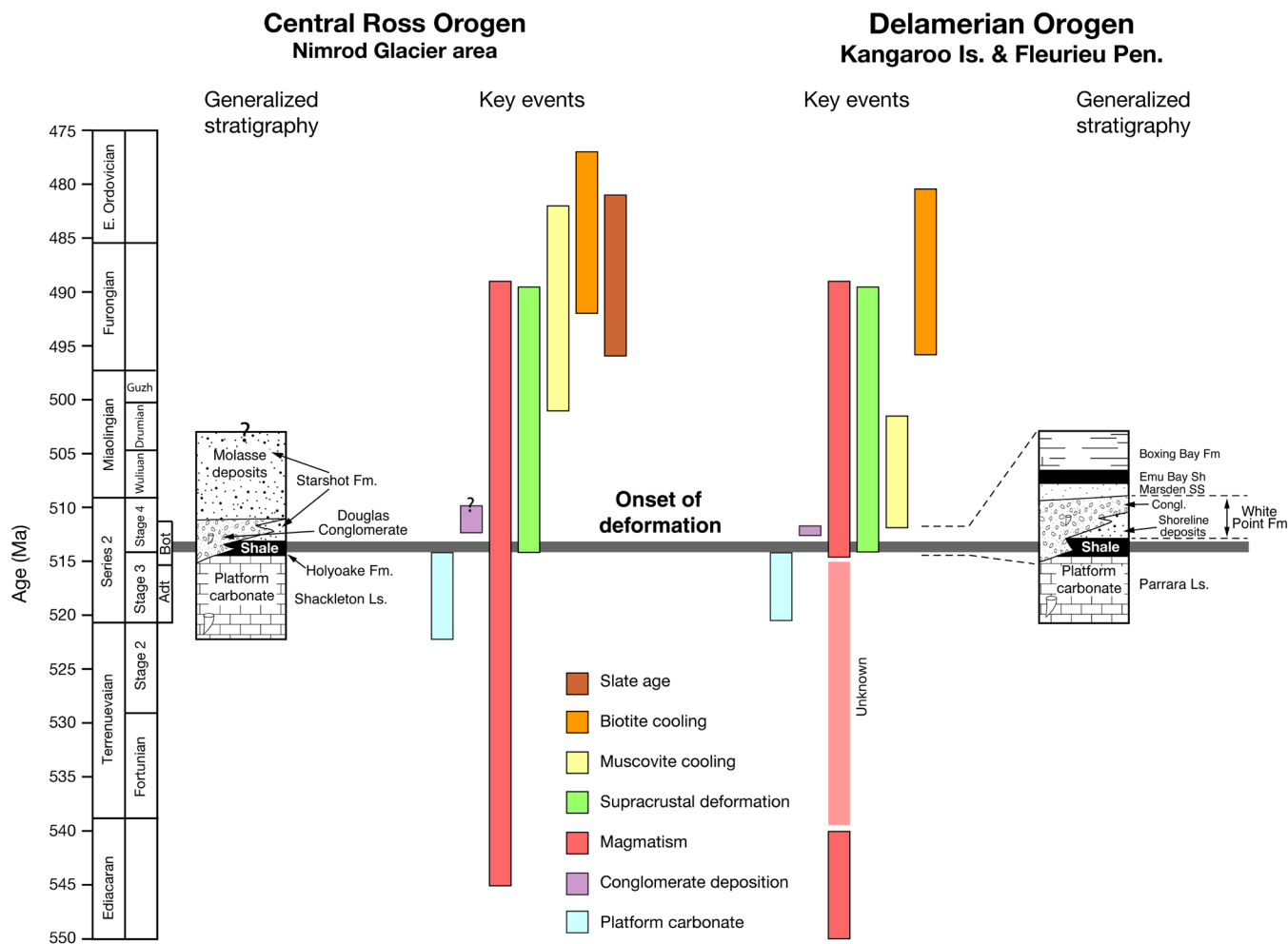


**Fig. 4. Time correlation diagram comparing Cambrian events in central Ross and Delamerian orogens.** Timescale shows series and stages, and Atdabanian and Botoman trilobite divisions for comparison. Schematic stratigraphic columns show primary depositional relations between biostratigraphically designated units (*16, 17, 31, 32, 36*), and colored bars denote time span of key events constrained by geochronological data (*18–21, 44, 45*). Note similar successions of archaeocyathid reefal carbonate, to black shale, and shallow-water sandstone, all down-cut and overlain by carbonate-clast conglomerate. Orogenic magmatism occurred through this period, but punctuated termination of carbonate deposition, shoaling, and overlap by prograding alluvial fanglomerate marks onset of supracrustal deformation in both areas. Syn- to post-orogenic cooling of micas and slates in metasedimentary lithologies mark metamorphism associated with structural shortening and thickening. Fm, Formation; Ls, Limestone.

(i) the deformation, as constrained by fossil ages and thermochronology, (ii) the base of Stage 4 (however defined), and (iii) the associated Sinsk event, all took place between ~514 and ~512 Ma.

The orogenic assembly of Gondwana was largely concluded by ~540 to 530 Ma, although some deformation and metamorphism continued afterward (48). Assembly was quickly followed by orogenic collapse, lithospheric extension, plutonism, and tectonic basin formation both along the East African–Antarctic Orogen and within intracratonic areas of Africa and Australia (9, 49–52). As discussed below, key geologic events signifying post-orogenic collapse within Gondwana's interior are dated to 518 to 510 Ma. Several examples of crustal extension of the interior of Gondwana are known, including migmatites and granitoids containing late-stage, post-collisional extensional structures in the Lurio Belt of Mozambique that formed between 518 and 514 Ma (53). There, Neoproterozoic clastic rocks of the Mecubúri Group were deposited in small fault-bounded intermontane basins formed during early stages of post-collisional orogen collapse (52). Overlying siliciclastic strata have a maximum depositional age of ~530 Ma based on detrital zircon analysis, and they were subject to medium-grade metamorphism and migmatization by 514 Ma (52). These rocks are, in turn, intruded by ~510-Ma granitoids (50). Younger mineral cooling ages indicate a long period of slow cooling attributed to mantle upwelling triggered by lithospheric delamination following Gondwana consolidation (53). The elevated temperatures, cooling age patterns, and extensional features together point to localized late-stage collapse by reactivation along orogenic structures formed during lithospheric thickening. Similarly, metamorphic granulites in Madagascar record high-temperature/low-pressure cooling trajectories as young as 510 Ma, attributed to orogenic collapse and crustal extension following earlier collision within the East African Orogen (9).

In the Dronning Maud Land area of East Antarctica, Pan-African convergence marking collisional orogenesis between East and West Gondwana was likewise followed by crustal extension, thought to represent orogenic collapse (49). In this region, referred to broadly as the East African–Antarctica Orogen, the post-collisional response is dated to ~530 to 510 Ma and is characterized by large-scale extensional structures and intrusion of voluminous granitoids. Emplacement of late syn- to post-tectonic intrusions coincided with retrograde metamorphism characterized by simultaneous cooling and decompression during extensional exhumation, probably triggered by the collapse of overthickened crust. Similar deep-crustal responses to orogenic collapse are known from other parts of the East African Orogen, such as in western Madagascar and the northern Arabian-Nubian Shield (9).

Another signature of post-orogenic lithospheric extension is development of large igneous provinces (LIPs). Magmatic activity in western Australia within the Kalkarindji continental flood basalt province included intrusion of dikes and diabase sills associated with the Officer, Wiso, and Georgina basins, dated by baddeleyite and zircon U-Pb to ~511 Ma (54), and eruption of subalkaline flood basalts of the Antrim Plateau Volcanics with $^{40}Ar/^{39}Ar$ ages of 513 to 498 Ma (55). Geochemical modeling of melt compositions in the Antrim Plateau and Table Hill volcanics indicates that a mantle plume was not required to induce melting but rather that post-orogenic thinning of Gondwana lithosphere may have triggered decompression melting of subcontinental lithospheric mantle and focused edge-driven asthenospheric convection into cratonic keels formed between higher-level basins (56). Other magmatism at this time included emplacement of

dikes and minor volcanic rocks in western Australia at 513 to 508 Ma (55, 57) and elsewhere in the North Australian Craton (58). Together, a decompressional melting scenario requires that extension leading to this middle Cambrian magmatism occurred before ~510 Ma.

The tectonic, magmatic, and depositional activity outlined here signifies a period of widespread lithospheric extension associated with orogenic collapse of the Gondwana interior that began nearly synchronously with the pulse of supracrustal contractional deformation along the peri-Gondwana margin described above that is biostratigraphically dated to ~514 to ~512 Ma. The erosional response to this deformation is also associated with the demise of carbonate platforms along much of its length. We therefore argue here for a causal linkage between post-orogenic extension in the hinterland interior of Gondwana driven by gravitational collapse of over-thickened lithosphere and a pulse and/or acceleration of shortening in the external convergent-margin realm. The body forces associated with supercontinent amalgamation, collision, over-thickening, collapse, and regional lithospheric extension documented within contiguous parts of Gondwana provide both a mechanism and the timing to explain the episode of active-margin deformation described here. Thus, we posit that an abrupt tectonic regime change within Gondwana's interior triggered a shift in convergent-margin deformation and magmatism along nearly the entire Australian and Antarctic outer margins. Furthermore, these tectonic responses are also linked to widely recognized paleoenvironmental changes and a biotic crisis in shallow water Cambrian settings.

The Ross and Delamerian orogens record W-dipping Gondwana-margin plate convergence by at least 550 Ma in the latest Neoproterozoic (Fig. 1) (10, 15, 19, 20, 59), yet a major change occurred in the early Cambrian. By this time, both the Ross and Delamerian systems were characterized by left-oblique, continental-margin plate convergence, dominantly I-type arc magmatism, medium-pressure Barrovian metamorphism, and Cambrian Stage 3 carbonate platform deposition (Fig. 4) (10, 15, 18, 20, 59, 60). These areas straddled the mid–Series 2 tropics (Fig. 1), promoting carbonate growth in shallow forearc settings that may have fostered shallow-water biotic radiation (33, 61). Deformation in Antarctica between 550 and 515 Ma was limited to inboard magmatism and incipient thickening of rift-margin deposits. In both areas, separated by ~1800 km at the time, an abrupt and simultaneous pulse of contractional deformation took place in active-margin supracrustal successions deposited originally within rift-margin and platformal settings (Figs. 2 and 4). A distinctive change in Cambrian plate-margin tectonic patterns is particularly well-preserved in Antarctica where abrupt cessation of carbonate deposition and drowning of archaeocyathid–microbial reefs reflected a pulse of subsidence, driven by thrust loading of crust from the west (Fig. 5). Subsequent development of coarse alluvial fans included initial erosion of basement sources and later erosion of deformed carbonate strata and the contemporaneous magmatic arc to the west (Fig. 5). Syn- to post-orogenic cooling ages of muscovite, biotite, and slate that range into the Ordovician document the response to crustal shortening and thickening (Fig. 4). A similar record is preserved in the Kangaroo Island succession and other parts of the Delamerian Orogen as discussed above, yet deformation there is west-vergent (34).

Despite their differences in deformation pattern, eastward forearc-directed thrusting in the Transantarctic Mountains (17) versus cratonward foreland thrusting on Kangaroo Island (34), both areas record near-synchronous (within a specific biostratigraphic zone) supracrustal shortening, a surficial response to punctuated tectonism
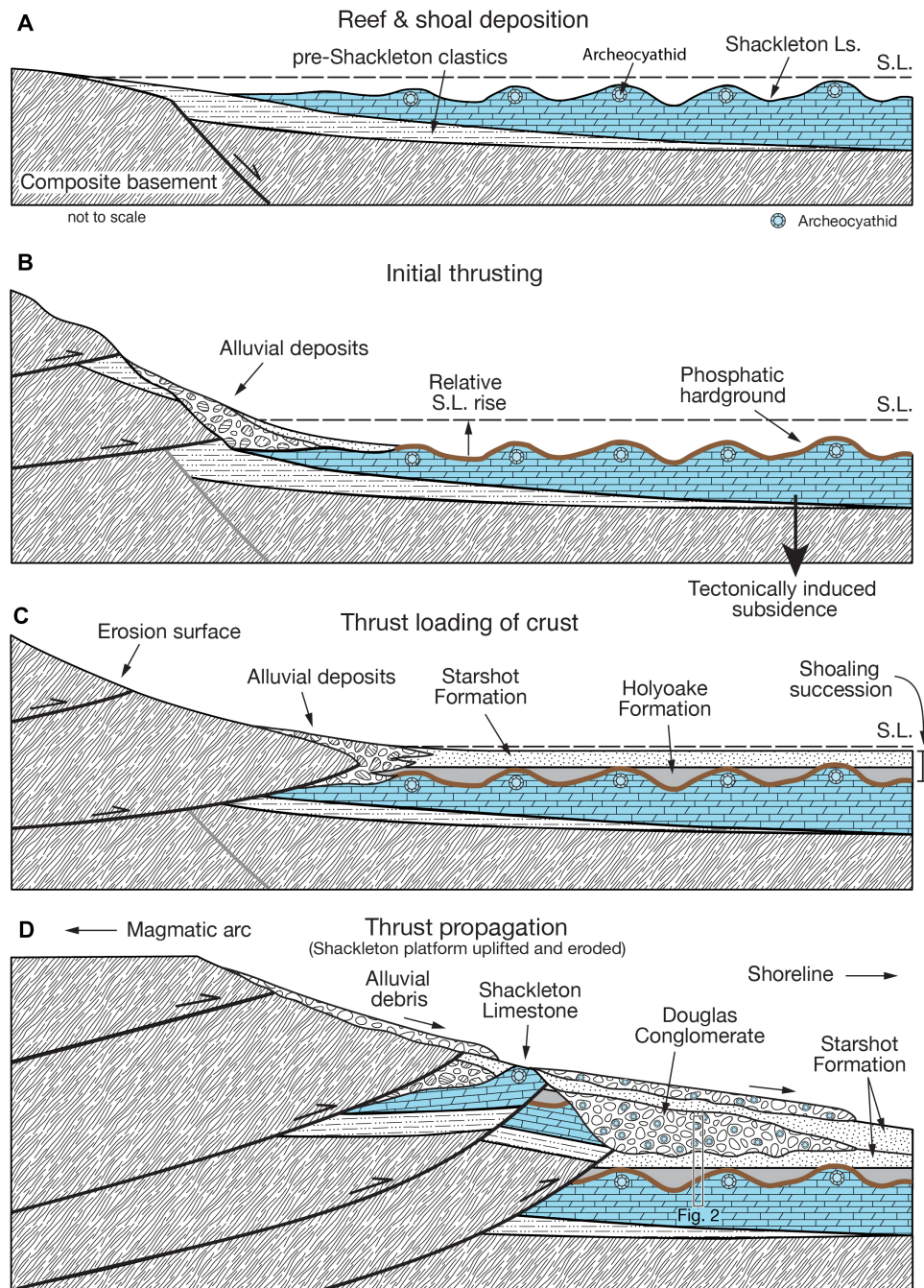
**Fig. 5. Model depicting sedimentary and structural evolution of central Ross Orogen during Cambrian late Series 2.** (**A**) Reef and shoal deposition phase, dominated by carbonate buildup (Shackleton Limestone) over older siliciclastic strata. Undifferentiated basement includes metamorphic rocks and Neoproterozoic Beardmore Group. Outboard subduction operated at this time (*14*). S.L., sea level. (**B**) Initial thrusting phase, in which inland basement was uplifted and eroded, and marine platform underwent initial tectonically induced subsidence, resulting in deepening and development of a capping phosphatic hardground (heavy brown line). (**C**) Ongoing oceanward thrust displacement led to further crustal loading and deposition of a clastic shoaling succession, including nodular shale (Holyoake Formation) and shallow-marine sandstone (Starshot Formation). Subaerial alluvial-fan deposits sourced from inland thrust sheets were dominated by basement debris. (**D**) Mature thrust propagation phase, in which forward-propagating thrusts cut into Shackleton Limestone, producing carbonate-clast debris containing archaeocyathid fossils. Ongoing erosion, transport, and alluvial deposition led to accumulation of coarse alluvial-fan deposits (Douglas Conglomerate). Narrow vertical rectangle in (D) corresponds to stratigraphic section in Fig. 2. Primary field relations, sedimentation patterns, faunal occurrences, and geochronological constraints provided by earlier studies (*16*, *17*, *23*, *95*).

that precisely captures the rapid onset of accelerated plate-margin convergence. Both areas later evolved toward younger upper-plate extension from ~500 to 480 Ma (*15*, *19*, *59*).

Beyond the coincident timing, however, contrasting structural styles in these two areas provide insight into their respective responses. Differences in sedimentation and deformation patterns in the two areas are likely due to the primary configuration of the Neoproterozoic rift margin, with the southern Australian margin developed as a broader basin system constructed upon extended Paleoproterozoic cratonic basement, whereas the Antarctic rift margin was narrower, and its sedimentary succession was less voluminous (Fig. 1). During subsequent plate-margin deformation, the Ross Orogen in the central Transantarctic Mountains behaved as a cratonal promontory, whereas the Delamerian belt evolved in a trough-like reentrant resembling an aulacogen at the edge of a long-lived Neoproterozoic basin (*15*, *30*, *34*). These inherited continental margin geometries led to earlier termination of Ross deformation by ~480 Ma, whereas progressively outboard orogenic activity persisted in the outer Tasmanides between ~485 and 340 Ma in the Lachlan Fold Belt (Fig. 1) (*62*). In addition to duration, plate margin activity also differed in character, in which the southern to central coast of Antarctica was dominated by Andean-type continental-margin magmatism with pronounced crustal thickening and high-pressure metamorphism (from at least 540 to 515 Ma) (*15*), while the region from northern Victoria Land northward into Australia was dominated by early Paleozoic supra-subduction–zone arc volcanism and marginal-basin development typical of accretionary orogens between at least 515 to 340 Ma (Fig. 1) (*62*). Despite these differences, the synchronous early Cambrian sedimentary patterns in these disparate areas attest to a near-simultaneous surficial response to tectonism across the broader Ross-Delamerian system.

The events highlighted here may also be expressed in a cryptic Cambrian succession in the Shackleton Range (Fig. 1), where conglomerate of the Mount Wegener Formation contains carbonate clasts with *P. janeae* Zone archaeocyathids, indicating syn-orogenic erosion and deposition during early Stage 4 or younger (<514 Ma) (*63*). Although the platform source for the limestone clasts is not exposed, conglomerate deposition is linked to collisional convergence of East and West Gondwana during closure of the Mozambique Ocean, consistent with Gondwana supercontinent consolidation as the cause of erosion, sedimentation, and marine habitat loss. The coincident timing of events in the Shackleton Range suggest that much of the Austral-Antarctic margin was marked by regional tectonic disruption of Series 2 carbonate depositional systems.

It is not possible to make a direct kinematic link between tectonic events of the Austral-Antarctic margin and eastern Gondwanan interior, as discussed here, and other Cambrian events on the western Gondwanan margin, yet several events recognized in west Gondwana have similar timing and may represent far-field tectonic responses of the former. These include (i) termination of the Pampean Orogeny ~515 Ma (*64*) and (ii) both initiation of subduction beneath West Ganderia [~515 Ma; (*65*)] and associated back-arc extension within that continent, causing rift separation of Ganderia and Amazonia during opening of the Rheic Ocean at ~510 Ma (*66*). Together, these events likely reflect supercontinental responses to post-Gondwana global tectonic reorganization in the Cambrian that have recognizable paleoenvironmental and paleobiological effects.

The timing of the tectonic event that we document here for the Austral-Antarctic margin of Gondwana corresponds with that of the Sinsk event (*2*, *3*). We posit that tectonic transformation involving inversion from collisional supercontinent assembly to lithospheric-scale orogenic collapse and extension triggered a series of cascading environmental and biotic processes during the Sinsk event. Widespread extension during this transformation, possibly associated with lithospheric delamination and/or mantle upwelling (*56*), was likely linked to a synchronous and/or immediately subsequent extrusion of the oldest LIP of the Phanerozoic in north-central Australia, the Kalkarindji continental basalts. Geochronological data constrain the onset of Kalkarindji eruptions to mid–Series 2. Zircon and baddeleyite U-Pb ages of 510.7 ± 0.6, 511 ± 5, and 508 ± 5 Ma were obtained from Kalkarindji dikes (*54*, *57*). Plagioclase $^{40}$Ar/$^{39}$Ar ages, including some recalculated results, from Kalkarindji dikes and volcanics of the Antrim Plateau Volcanic rock suite range from 512.8 ± 1.6 to 508.7 ± 4.3 Ma (*55*). Given reported uncertainties, the oldest possible magmatic ages are 516 to 514 Ma. Published radiometric ages and associated uncertainties for the Kalkarindji LIP indicate that emplacement took place through much of Cambrian Series 2, with many dates in the range of 514 to 508 Ma (*54*, *55*). Integration of all ages indicates that initial Kalkarindji LIP emplacement likely took place as early as 514 to 513 Ma (see the Supplementary Materials). This is in the same age range as the tectonic transition of the Austral-Antarctic margin of Gondwana described here, during which time the Kalkarindji magmatism may plausibly have contributed volatile and aerosol emissions, affecting atmospheric change in Cambrian Series 2. The eroded remains of the Kalkarindji basalt province cover 55,000 km (*2*, *58*, *67*, *68*). Its estimated volume of ~$1.5 \times 10^5$ km (*3*, *69*) could have released as much as ~2% of the Cambrian atmospheric $CO_2$ load (*58*), and, coupled with the simultaneous release of large amounts of $CH_4$ and $SO_2$ emissions, it led to rapid climatic changes and environmental pressures (*54*, *70*), specifically expressed as the Sinsk event.

Climate change at this time is supported by two major perturbations of the carbon cycle, namely, (i) a negative δ (*13*) $C_{carb}$ shift near or at the base of Stage 4, the Botoman-Toyonian Extinction (BTE) interval, and the events outlined in this study; and (ii) isotope anomaly ROECE, which corresponds with the Series 2–Miaolingian boundary Redlichiid–Olenellid Extinction (*71–76*) and the main phase of Kalkarindji volcanism at ~509 Ma (*67–70*). Two different isotopic features have been placed at the base of Stage 4: the Archaeocyathid Extinction Carbon Isotope Excursion negative excursion (*73*) and the initiation point of the underlying MICE positive excursion (*72*). Regardless of which is best placed at the base of Stage 4, that isotopic feature and the BTE interval correspond to the Sinsk event (*1*, *2*), the first major extinction of the Cambrian. The Sinsk records a global genus-level reduction in diversity of ~45% (*77*), reduction of body sizes of many marine invertebrate groups (*4*), a major extinction of archaeocyathan reefs (*78*), elevated sea surface temperatures (*79*), a global greenhouse climate (*2*, *80*), extensive deposition of evaporites (*81*), and spread of anoxic deep waters into shallow-water environments (*1–3*, *82*). This is reflected in the rapid demise of archaeocyathid species in South Australia from 100+ reef-building species on carbonate platforms during Stages 3 to 4 (*83*) to only three to four species before their final extinction in late Stage 4 shallow water carbonate (*84*). Although authors have opined on causalities between the Kalkarindji LIP, climate change, and extinction (*54*, *70*), some have been hesitant to link the LIP to extinction (*58*). One possible link is that warming caused by the release of volatile emissions through volcanism may have elevated sea surface temperatures and led to reduced oceanic turnover, stratification, and bottom water anoxia, the latter causing dysoxia and elevated rates of extinction (*85*). A sea level rise,

starting at the base of Stage 4 (*86*), could also have been an important factor in the extinction, particularly as sea level rise produced by elevated atmospheric and ocean temperatures could have led to drowning of continental interiors with oxygen-deficient waters.

Our hypothesis that the initiation of supracrustal Ross Orogenic activity, Sinsk event extinction, and initial Kalkarindji LIP extrusion and associated effects were nearly synchronous is highly dependent on the precision of the absolute age constraints for these events. The tectonic activity and the Sinsk event both took place within the *P. janeae* trilobite Zone (Fig. 6). Their age is bracketed by strata from upper Stage 3 in Britain (W. Avalonia), below the *P. janeae* Zone, which yielded an age of 514.45 ± 0.36 Ma (*46*), and a radiometric date on strata from the middle to upper *P. janeae* Zone (Billy Creek Formation of Australia) that places an upper constraint for these events at 511.87 ± 0.14 Ma (*47*).

Age models for the Sinsk event (*3*, *87*) rest largely on radiometric dates, chemostratigraphic curves, and estimates of accumulation rates. The timing of the Sinsk event will be close to, or at, the base of Stage 4 (and the *P. janeae* Zone); however, the stage boundary is ultimately defined. The event is recorded in strata directly above a sequence boundary at the base of the Sinsk Formation in Siberia. The amount of time represented by that sequence boundary is unknown, so the Sinsk could be a million years or more younger than the 514.45 ± 0.36 Ma (*46*) radiometric date. As a result, the dates (with errors) of initial LIP activity are well within the range of possible dates for the Sinsk event. Our suggestion that tectonics triggered a series of events that resulted in the Sinsk extinction is a hypothesis that can be tested with future geochronologic data, although the present overlap of geochronologic ages for LIP initiation (514 to 513 Ma) and the maximum age for upper Stage 3 (~514.5 Ma) strongly supports the hypothesis. In addition to the effects of widespread oceanic anoxia on marine fauna during the Sinsk event, we suggest that onset of supracrustal tectonic deformation led to widespread loss of shallow water carbonate habitats of eastern Gondwana (Australian and Antarctic margins) and possibly much of the perimeter of the supercontinent. This occurred through both initial thrust-loading–induced marine subsidence, focused at the convergent plate boundary, and subsequent uplift and erosion of carbonate platforms. Such loss of habitat may have added to the overall biotic stresses of the Sinsk event and to global extinction patterns, given the
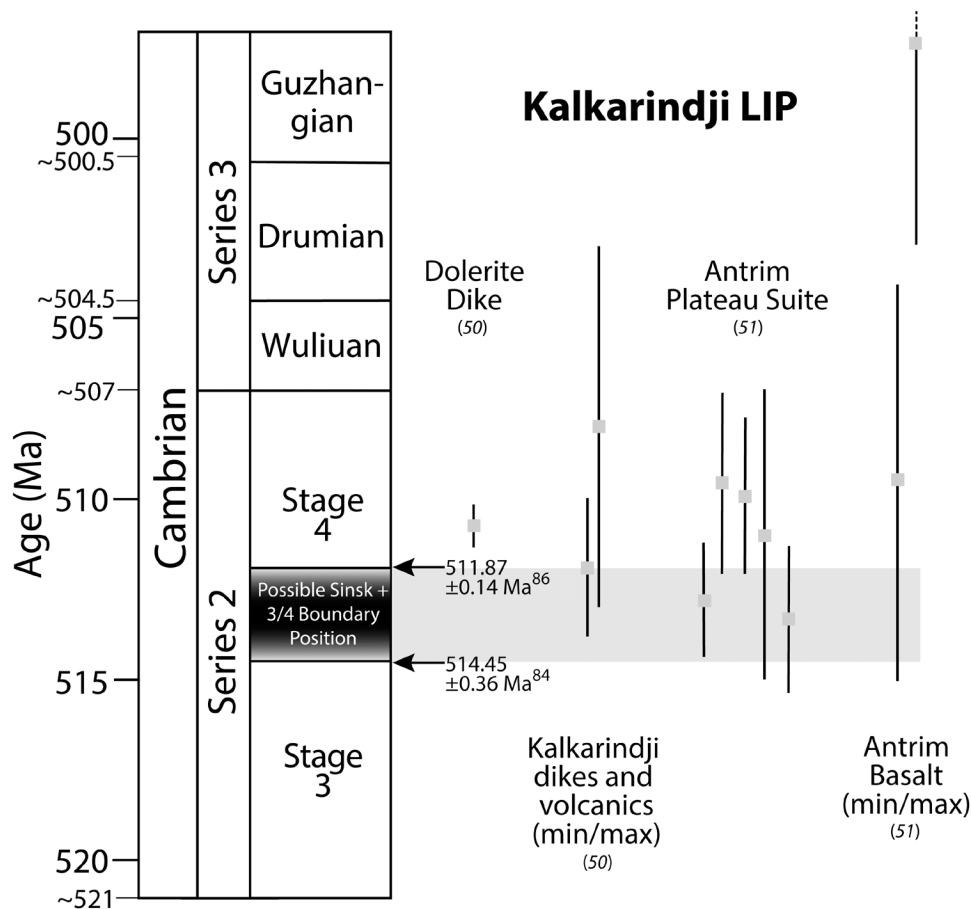


**Fig. 6. Time diagram for the Cambrian, showing the oldest and youngest possible age of the Sinsk event and the Stage 3 to 4 boundary (black arrows with radiometric dates).** The base of Stage 4 and the *P. janeae* Zone is younger than 514.45 ± 0.36 Ma; the date of 511.87 ± 0.14 from the middle to upper *P. janeae* Zone is the upper limit for both the Sinsk and the supracrustal deformation event described herein. Dated units from the Kalkarindji LIP in Australia are shown as gray squares with error bars. Two ages from both the Kalkarindji dikes/volcanics and Antrim basalt represent minimum and maximum ages. The time span during which tectonic shortening occurred along the Ross-Delamerian margin of Antarctica and Australia, and during which the Sinsk event took place, is shown as a horizontal gray band. Sources of age data cited in Discussion.

extensive carbonate shelves around the supercontinent Gondwana that were potentially affected by the tectonic transition documented herein.

In summary, the tectono-sedimentary events along the Austral-Antarctic margin were part of a supercontinent-wide transformation that led to shallow-water carbonate habitat loss along equatorial Gondwana. These events were also geodynamically linked to a broad inversion from collisional supercontinental assembly to extensional tectonics associated with lithospheric-scale orogenic collapse within the interior of Gondwana, the latter including eruption of the Kalkar-indji LIP. The Kalkarindji LIP eruptions released considerable levels of atmospheric $CO_2$ and associated $CH_4$ and $SO_2$ emissions, all of which caused a series of cascading environmental processes that resulted in ocean warming, reduced oceanic turnover, widespread bottom-water anoxia in marginal and epicontinental seas, and, ultimately, the Sinsk extinction.

## MATERIALS AND METHODS

Specimens of trilobites were collected in situ from the Holyoake Formation during expeditions in 2000 and 2011. Those preserved in mudstone (Fig. 3, A and C to F) are weakly distorted with moderate convexity, while the one preserved in grainstone (Fig. 3B) is preserved with original convexity. The specimens of eodiscoids (Fig. 3, C to F) are external molds and latex casts were prepared. All specimens are reposited in the Cincinnati Museum, prefixed with CMC IP. Mechanical preparation of the *E. bilobata* specimens was done with an AUTOMEL Electric Engraver (Dong Yang Electric Co.).

Trilobite specimens were coated with magnesium oxide smoke. The specimens of *E. bilobata* were photographed with a Canon EOS 6D using a Canon EF 100 mm f/2.8 L IS USM macro lens. The eodiscoid fossils were photographed with a Leica M205C microscope equipped with a Leica DFC550 camera using the *z*-stacking method.

## Supplementary Materials

**This PDF file includes:**
Supplementary Materials

## REFERENCES AND NOTES

1. A. Y. Zhuravlev, R. A. Wood, Anoxia as the cause of the mid-Early Cambrian (Botomian) extinction event. *Geology* **24**, 311–314 (1996).
2. A. Y. Zhuravlev, R. A. Wood, The two phases of the Cambrian Explosion. *Sci. Rep.* **8**, 16656 (2018).
3. T. He, M. Zhu, B. J. W. Mills, P. M. Wynn, A. Y. Zhuravlev, R. Tostevin, P. A. E. Pogge von Strandmann, A. Yang, S. W. Poulton, G. A. Shields, Possible links between extreme oxygen perturbations and the Cambrian radiation of animals. *Nat. Geosci.* **12**, 468–474 (2019).
4. A. Y. Zhuravlev, R. A. Wood, Dynamic and synchronous changes in metazoan body size during the Cambrian Explosion. *Sci. Rep.* **10**, 6784 (2020).
5. P. A. Cawood, R. A. Strachan, S. A. Pisarevsky, D. P. Gladkochub, J. B. Murphy, Linking collisional and accretionary orogens during Rodinia assembly and breakup: Implications for models of supercontinent cycles. *Earth Planet. Sci. Lett.* **449**, 118–126 (2016).
6. J. G. Meert, A synopsis of events related to the assembly of eastern Gondwana. *Tectonophysics* **362**, 1–40 (2003).
7. R. J. Stern, Arc assembly and continental collision in the Neoproterozoic East-African Orogen: Implications for the consolidation of Gondwanaland. *Annu. Rev. Earth Planet. Sci.* **22**, 319–351 (1994).
8. J. Jacobs, C. M. Fanning, F. Henjes-Kunst, M. Olesch, H. J. Paech, Continuation of the Mozambique Belt into East Antarctica: Grenville-age metamorphism and polyphase Pan-African high-grade events in Central Dronning Maud Land. *J. Geol.* **106**, 385–406 (1998).
9. H. Fritz, M. Abdelsalam, K. A. Ali, B. Bingen, A. S. Collins, A. R. Fowler, W. Ghebreab, C. A. Hauzenberger, P. R. Johnson, T. M. Kusky, P. Macey, S. Muhongo, R. J. Stern, G. Viola,

10. Orogen styles in the East African Orogen: A review of the Neoproterozoic to Cambrian tectonic evolution. *J. Afr. Earth Sci.* **86**, 65–106 (2013).
10. P. A. Cawood, Terra Australis Orogen: Rodinia breakup and development of the Pacific and Iapetus margins of Gondwana during the Neoproterozoic and Paleozoic. *Earth-Sci. Rev.* **69**, 249–279 (2005).
11. P. M. Myrow, N. C. Hughes, N. R. McKenzie, Cambrian–Ordovician orogenesis in Himalayan equatorial Gondwana. *Geol. Soc. Am. Bull.* **128**, 1679–1695 (2016).
12. P. M. Myrow, N. C. Hughes, N. R. McKenzie, Reconstructing the Himalayan margin prior to collision with Asia: Proterozoic and lower Paleozoic geology and its implications for Cenozoic tectonics in P.J. Treloar, M.P. Searle, Eds. *Himalayan Tectonics: A Modern Synthesis. J. Geol. Soc. (London, U. K.) Spec. Pub.* **483**, 39–64 (2019).
13. N. R. McKenzie, N. C. Hughes, B. C. Gill, P. M. Myrow, Plate tectonic influences on Neoproterozoic–Early Paleozoic climate and animal evolution. *Geology* **42**, 127–130 (2014).
14. T. W. Wong Hearing, A. Pohl, M. Williams, Y. Donnadieu, T. H. P. Harvey, C. R. Scotese, P. Sepulchre, A. Franc, T. R. A. Vandenbroucke, Quantitative comparison of geological data and model simulations constrains early Cambrian geography and climate. *Nat. Commun.* **12**, 3868 (2021).
15. J. W. Goodge, Geological and tectonic evolution of the Transantarctic Mountains, from ancient craton to recent enigma. *Gondw. Res.* **80**, 50–122 (2020).
16. P. M. Myrow, M. C. Pope, J. W. Goodge, W. Fischer, A. R. Palmer, Depositional history of pre-Devonian strata and timing of Ross Orogenic tectonism in the central Transantarctic Mountains. Antarctica. *Geol. Soc. Am. Bull.* **114**, 1070–1088 (2002).
17. J. W. Goodge, P. Myrow, D. Phillips, C. M. Fanning, I. S. Williams, Siliciclastic record of rapid denudation in response to convergent-margin orogenesis, Ross Orogen, Antarctica, in M. Bernet, C. Spiegel, Eds. Detrital Thermochronology—Provenance Analysis, Exhumation, and Landscape Evolution of Mountain Belts. *Geol. Soc. Am. Spec. Paper Boulder, Colorado* **378**, 101–122 (2004a).
18. J. W. Goodge, I. S. Williams, P. Myrow, Provenance of Neoproterozoic and lower Paleozoic siliciclastic rocks of the Central Ross Orogen, Antarctica: Detrital record of rift-, passive- and active-margin sedimentation. *Geol. Soc. Am. Bull.* **116**, 1253–1279 (2004).
19. J. Foden, M. A. Elburg, J. Dougherty-Page, A. Burtt, The timing and duration of the Delamerian Orogeny: Correlation with the Ross Orogen and implications for Gondwana assembly. *J. Geol.* **114**, 189–210 (2006).
20. J. Foden, M. Elburg, S. Turner, C. Clark, M. L. Blades, G. Cox, A. S. Collins, K. Wolff, C. George, Cambro-Ordovician magmatism in the Delamerian orogeny: Implications for tectonic development of the southern Gondwanan margin. *Gondw. Res.* **81**, 490–521 (2020).
21. S. Turner, T. Ireland, J. Foden, E. Belousova, G. Wörner, J. Keeman, A comparison of granite genesis in the Adelaide Fold Belt and Glenelg River Complex using U–Pb, Hf and O isotopes in zircon. *J. Petrol.* **63**, egac102 (2022).
22. J. W. Goodge, P. Myrow, I. S. Williams, S. A. Bowring, Age and provenance of the Beardmore Group, Antarctica: Constraints on Rodinia supercontinent breakup. *J. Geol.* **110**, 393–406 (2002).
23. M. N. Rees, A. J. Rowell, E. D. Cole, Aspects of the late Proterozoic and Paleozoic geology of the Churchill Mountains, southern Victoria Land. *Antarct. J. U. S.* **22**, 23–25 (1988).
24. M. N. Rees, B. R. Pratt, A. J. Powell, Early Cambrian reefs, reef complexes, and associated lithofacies of the Shackleton Limestone, Transantarctic Mountains. *Sedimentology* **36**, 341–361 (1989).
25. A. R. Palmer, A. J. Rowell, Early Cambrian trilobites from the Shackleton Limestone of the central Transantarctic Mountains. *J. Paleontol.* **69**, 1–28 (1995).
26. F. Debrenne, P. D. Kruse, Shackleton Limestone archaeocyaths. *Alcheringa* **10**, 235–278 (1986).
27. T. M. Claybourn, S. M. Jacquet, C. B. Skovsted, T. P. Topper, L. E. Holmer, G. A. Brock, Mollusks from the upper Shackleton Limestone (Cambrian Series 2), Central Transantarctic Mountains, East Antarctica. *J. Paleontol.* **93**, 437–459 (2019).
28. T. M. Claybourn, C. B. Skovsted, L. E. Holmer, B. Pan, P. M. Myrow, T. P. Topper, G. A. Brock, Brachiopods from the Byrd group (Cambrian Series 2, Stage 4) central transantarctic mountains, East Antarctica: biostratigraphy, phylogeny and systematics. *Pap. Palaeontol.* **6**, 349–383 (2020).
29. T. M. Claybourn, C. B. Skovsted, M. J. Betts, L. E. Holmer, L. Bassett-Butt, G. A. Brock, Camenellan tommotiids from the Cambrian Series 2 of East Antarctica: Biostratigraphy, palaeobiogeography, and systematics. *Acta Palaeontol. Pol.* **66**, 207–229 (2021).
30. W. V. Preiss, The Adelaide Geosyncline of South Australia and its significance in Neoproterozoic continental reconstruction. *Precambrian Res.* **100**, 21–63 (2000).
31. J. G. Gehling, J. B. Jago, J. R. Paterson, D. C. García-Bellido, G. D. Edgecombe, The geological context of the ower Cambrian (Series 2) Emu Bay Shale Lagerstätte and adjacent stratigraphic units, Kangaroo Island, South Australia. *Aust. J Earth Sci.* **58**, 243–257 (2011).
32. P. D. Kruse, E.-E. Moreno, Archaeocyaths of the White Point Conglomerate, Kangaroo Island, South Australia. *Alcheringa* **38**, 1–64 (2014).
33. G. A. Brock, M. J. Engelbretsen, J. B. Jago, P. D. Kruse, J. R. Laurie, J. H. Shergold, G. R. Shi, J. E. Sorauf, Palaeobiogeographic affinities of Australian Cambrian faunas. *Mem. Assoc. Australas. Palaeontol.* **23**, 1–61 (2000).

34. T. Flöttmann, P. Haines, J. Jago, P. James, A. Belperio, J. Gum, Formation and reactivation of the Cambrian Kanmantoo Trough, SE Australia: implications for early Palaeozoic tectonics at eastern Gondwana's plate margin. *J. Geol. Soc.* **155**, 525–539 (1998).

35. M. J. Betts, T. M. Claybourn, G. A. Brock, J. B. Jago, C. B. Skovsted, J. R. Paterson, Early Cambrian shelly fossils from the White Point Conglomerate, Kangaroo Island. *Acta Palaeontol. Pol.* **64**, 489–522 (2019).

36. B. Daily, P. S. Moore, B. R. Rust, Terrestrial–marine transition in the Cambrian rocks of Kangaroo Island, South Australia. *Sedimentology* **27**, 379–399 (1980).

37. D. I. Gravestock, C. G. Gatehouse, The Geology of South Australia, Volume 2, The Phanerozoic. *Geol. Surv. S. Aust. Bull.* **54**, 5–19 (1995).

38. R. J. F. Jenkins, M. Sandiford, Observations on the tectonic evolution of the southern Adelaide Fold Belt. *Tectonophysics* **214**, 27–36 (1992).

39. C. Nedin, Taphonomy of the Early Cambrian Emu Bay Shale Lagerstätte, Kangaroo Island, South Australia. *Bull. Nation. Mus. Nat. Sci.* **10**, 133–141 (1997).

40. A. P. Belperio, M. Fairclough, C. Gatehouse, J. Hough, W. Preiss, J. C. Gum, Tectonic and metallogenic framework of the Cambrian Stansbury Basin-Kanmantoo Trough, South Australia. *AGSO J. Aust. Geol. Geophys.* **17**, 183–200 (1998).

41. J. B. Jago, C. J. Bentley, J. R. Paterson, J. D. Holmes, T. R. Lin, X. W. Sun, The stratigraphic significance of early Cambrian (Series 2, Stage 4) trilobites from the Smith Bay Shale near Freestone Creek, Kangaroo Island. *Aust. J. Earth Sci.* **68**, 204–212 (2021).

42. J. R. Paterson, C. B. Skovsted, G. A. Brock, J. B. Jago, An early Cambrian faunule from the Koolywurtie Limestone Member (Parara Limestone), Yorke Peninsula, South Australia and its biostratigraphic significance. *Mem. Assoc. Australas. Palaeontol.* **34**, 131–146 (2007).

43. J. R. Paterson, D. C. García-Bellido, J. B. Jago, J. G. Gehling, M. S. Y. Lee, G. D. Edgecombe, The Emu Bay Shale *Konservat-Lagerstätte*: a view of Cambrian life from East Gondwana. *J. Geol. Soc.* **173**, 1–11 (2016).

44. J. W. Goodge, C. M. Fanning, M. D. Norman, V. C. Bennett, Temporal, isotopic and spatial relations of early Palaeozoic Gondwana-margin arc magmatism, central Transantarctic Mountains, Antarctica. *J. Petrol.* **53**, 2027–2065 (2012).

45. S. P. Turner, S. P. Kelley, A. H. M. VandenBerg, J. D. Foden, M. Sandiford, T. Flöttmann, Source of the Lachlan fold belt flysch linked to convective removal of the lithospheric mantle and rapid exhumation of the Delamerian-Ross fold belt. *Geology* **24**, 941–944 (1996).

46. T. H. P. Harvey, M. Williams, D. J. Condon, P. R. Wilby, D. J. Siveter, A. W. A. Rushton, M. J. Leng, S. E. Gabbott, A refined chronology for the Cambrian succession of southern Britain. *J. Geol. Soc.* **168**, 705–716 (2011).

47. M. B. Betts, J. R. Paterson, S. M. Jacquet, A. S. Andrew, P. A. Hall, J. B. Jago, E. A. Jagodzinski, W. V. Preiss, J. L. Crowley, S. A. Birch, C. P. Mathewson, D. C. García-Bellido, T. P. Topper, C. B. Skovsted, G. A. Brock, Early Cambrian chronostratigraphy and geochronology of South Australia. *Earth-Sci. Rev.* **185**, 498–543 (2018).

48. P. A. Cawood, C. Buchan, Linking accretionary orogenesis with supercontinent assembly. *Earth Sci. Rev.* **82**, 217–256 (2007).

49. J. Jacobs, R. Klemd, C. M. Fanning, W. Bauer, F. Colombo, Extensional collapse of the late Neoproterozoic-early Palaeozoic East African-Antarctic Orogen in central Dronning Maud Land, East Antarctica. *Geol. Soc. Spec. Pub.* **206**, 271–287 (2003).

50. J. Jacobs, B. Bingen, R. J. Thomas, W. Bauer, M. T. D. Wingate, P. Feitio, Early Palaeozoic orogenic collapse and voluminous late-tectonic magmatism in Dronning Maud Land and Mozambique: insights into the partially delaminated orogenic root of the East African-Antarctic Orogen? In: M. Satish-Kumar, Y. Motoyoshi, Y. Osanai, Y. Hiroi, K. Shiraishi, Eds. *Geodynamic Evolution of East Antarctica: A Key to the East–West Gondwana Connection*. *Geol. Soc. Lon. Spec. Pub.* **308**, 69–90 (2008).

51. G. Viola, I. H. C. Henderson, B. Bingen, R. J. Thomas, M. A. Smethurst, S. de Azavedo, Growth and collapse of a deeply eroded orogen: Insights from structural, geophysical, and geochronological constraints on the Pan-African evolution of NE Mozambique. *Tectonics* **27**, TC5009 (2008).

52. R. J. Thomas, J. Jacobs, M. S. A. Horstwood, K. Ueda, B. Bingen, R. Matola, The Mecubúri and Alto Benfica Groups, NE Mozambique: Aids to unravelling ca. 1 and 0.5Ga events in the East African Orogen. *Precambrian Res.* **178**, 72–90 (2010).

53. K. Ueda, J. Jacobs, R. J. Thomas, J. Kosler, F. Jourdan, R. Matola, Delamination-induced late-tectonic deformation and high-grade metamorphism of the Proterozoic Nampula Complex, northern Mozambique. *Precambrian Res.* **196-197**, 275–294 (2012).

54. F. Jourdan, K. Hodges, B. Sell, U. Schaltegger, M. T. D. Wingate, L. Z. Evins, U. Söderlund, P. W. Haines, D. Phillips, T. Blenkinsop, High-precision dating of the Kalkarindji large igneous province, Australia, and synchrony with the Early–Middle Cambrian (Stage 4–5) extinction. *Geology* **42**, 543–546 (2014).

55. P. E. Marshall, A. M. Halton, S. P. Kelley, M. Widdowson, S. C. Sherlock, New40Ar/39Ar dating of the Antrim Plateau Volcanics, Australia: clarifying an age for the eruptive phase of the Kalkarindji continental flood basalt province. *J. Geol. Soc.* **175**, 974–985 (2018).

56. B. D. Ware, F. Jourdan, R. Merle, M. Chiaradia, K. Hodges, The Kalkarindji Large Igneous Province, Australia: Petrogenesis of the oldest and most compositionally homogeneous province of the Phanerozoic. *J. Petrol.* **59**, 635–665 (2018).

57. F. A. Macdonald, M. T. D. Wingate, K. Mitchell, Geology and age of the Glikson impact structure, Western Australia. *Aust. J. Earth Sci.* **52**, 641–651 (2005).

58. P. E. Marshall, L. E. Faggetterand, M. Widdowson, Was the Kalkarindji continental flood basalt province a driver of environmental change at the dawn of the Phanerozoic?, in *Large Igneous Provinces: A Driver of Global Environmental and Biotic Changes.*, R. E. Ernst, A. J. Dickson, A. Bekker, Eds. (Geophysical Monograph Series, American Geophysical Union, Washington D.C., 2021), pp.435–447.

59. A. I. S. Kemp, C. J. Hawkesworth, W. J. Collins, C. M. Gray, P. L. Blevin, Isotopic evidence for rapid continental growth in an extensional accretionary orogen: The Tasmanides, eastern Australia. *Earth Planet. Sci. Lett.* **284**, 455–466 (2009).

60. J. W. Goodge, V. L. Hansen, S. M. Peacock, B. K. Smith, N. W. Walker, Kinematic evolution of the Miller Range shear zone, central Transantarctic Mountains, Antarctica, and implications for Neoproterozoic to Early Paleozoic tectonics of the East Antarctic Margin of Gondwana. *Tectonics* **12**, 1460–1478 (1993).

61. I. W. D. Dalziel, Cambrian transgression and radiation linked to an Iapetus-Pacific oceanic connection? *Geology* **42**, 979–982 (2014).

62. R. A. Glen, The Tasmanides of eastern Australia, In: A. P. M. Vaughan, P.T. Leat, R.J. Pankhurst, Eds. *Terrane Processes at the Margins of Gondwana*. *Geol. Soc. Lon. Spec. Pub.* **246**, 23–96 (2005).

63. M. Rodríguez-Martínez, W. Buggisch, S. Menéndez, E. Moreno-Eiris, A. Perejón, Reconstruction of a Ross lost Cambrian Series 2 mixed siliciclastic–carbonate platform from carbonate clasts of the Shackleton Range, Antarctica. *Earth Environ. Sci. Trans. R. Soc. Edinburgh* **113**, 175–226 (2022).

64. V. A. Ramos, M. Escayola, P. Leal, M. M. Pimentel, J. O. S. Santos, The late stages of the Pampean Orogeny, Córdoba (Argentina): Evidence of postcollisional Early Cambrian slab break-off magmatism. *J. South Am. Earth Sci.* **64**, 351–364 (2015).

65. C. R. van Staal, S. M. Barr, J. W. F. Waldron, D. I. Schofield, A. Zagorevski, C. E. White, Provenance and Paleozoic tectonic evolution of Ganderia and its relationships with Avalonia and Megumia in the Appalachian-Caledonide orogen. *Gondw. Res.* **98**, 212–243 (2021).

66. H. Sandeman, V. McNicoll1, D. T. W. Evans, U-Pb geochronology and lithogeochemistry of the host rocks to the Reid gold deposit, Exploits Subzone- Mount Cormack subzone boundary area, central Newfoundland. *Current Research Newfoundland and Labrador Department of Natural Resources Geological Survey Report* **12-1**, 85–102 (2012).

67. R. J. Bultitude, The Antrim Plateau Volcanics, Victoria River District, Northern Territory. *Bur. Mineral Resources, Geol. Geophys.* **1971/69**, (1971).

68. R. J. Bultitude, The Geology and Petrology of the Helen Springs, Nutwood Downs, and Peaker Piker Volcanics. *Bur. of Mineral Resources, Geol. Geophys.* **1972/74**, (1972).

69. P. E. Marshall, M. Widdowson, D. T. Murphy, The Giant Lavas of Kalkarindji: Rubbly pāhoehoe lava in an ancient continental flood basalt province. *Palaeogeogr. Palaeoclimatol. Palaeoecol.* **441**, 22–37 (2016).

70. L. M. Glass, D. Phillips, The Kalkarindji continental flood basalt province: A new Cambrian large igneous province in Australia with possible links to faunal extinctions. *Geology* **34**, 461–464 (2006).

71. I. P. Montañez, J. L. Banner, D. A. Osleger, L. E. Borg, P. J. Bosserman, Integrated Sr isotope variations and sea-level history of Middle to Upper Cambrian platform carbonates: Implications for the evolution of Cambrian seawater $^{87}Sr/^{86}Sr$. *Geology* **24**, 917–920 (1996).

72. M. Y. Zhu, L. E. Babcock, S. C. Peng, Advances in Cambrian stratigraphy and paleontology: Integrating correlation techniques, paleobiology, taphonomy and paleoenvironmental reconstruction. *Palaeoworld* **15**, 217–222 (2006).

73. C. Chang, W. Hu, X. Wang, H. Yu, A. Yang, J. Cao, S. Yao, Carbon isotope stratigraphy of the lower to middle Cambrian on the eastern Yangtze Platform, South China. *Palaeogeogr. Palaeoclimatol. Palaeoecol.* **479**, 90–101 (2017).

74. L. E. Faggetter, "Environmental change, trilobite extinction and massive volcanism at the Cambrian Series 2-Series 3 boundary" thesis, University of Leeds (2017).

75. L. E. Faggetter, P. B. Wignall, S. E. Pruss, D. S. Jones, S. Grasby, M. Widdowson, R. J. Newton, Mercury chemostratigraphy across the Cambrian Series 2- Series 3 boundary: Evidence for increased volcanic activity coincident with extinction? *Chem. Geol.* **510**, 188–199 (2017).

76. Y. Ren, D. Zhong, C. Gao, T. Liang, H. Sun, D. Wu, X. Zheng, High-resolution carbon isotope records and correlations of the lower Cambrian Longwangmiao formation (stage 4, Toyonian) in Chongqing, South China. *Palaeogeogr. Palaeoclimatol. Palaeoecol.* **485**, 572–592 (2017).

77. J. J. Sepkoski, Patterns of Phanerozoic extinction: A perspective from global data bases, in *Global Events and Event Stratigraphy in the Phanerozoic* (Springer, 1996), pp. 35–51.

78. M. D. Brasier, The basal Cambrian transition and bio-events (from terminal Proterozoic extinctions to Cambrian biomeres), in *Global Events and Event Stratigraphy in the Phanerozoic* (Springer, 1996), pp. 113–138.

79. T. Wotte, C. B. Skovsted, M. J. Whitehouse, A. Kouchinsky, Isotopic evidence for temperate oceans during the Cambrian Explosion. *Sci. Rep.* **9**, 6330 (2019).

80. T. W. Hearing, T. H. P. Harvey, M. Williams, M. J. Leng, A. L. Lamb, P. R. Wilby, S. E. Gabbott, A. Pohl, Y. Donnadieu, An early Cambrian greenhouse climate. *Sci. Adv.* **4**, eaar5690 (2018).

81. M. Keller, J. D. Cooper, O. Lehnert, Sauk megasequence supersequences, southern Great Basin: second-order accommodation events in the southwest Cordilleran margin platform. *Am. Assoc. Petrol. Geol. Memoir* **98**, 873–896 (2012).

82. A. Y. Ivantsov, A. Y. Zhuravlev, A. V. Leguta, V. A. Krassilov, L. M. Melnikova, G. T. Ushatinskaya, Palaeoecology of the early Cambrian Sinsk biota from the Siberian platform. *Palaeogeogr. Palaeoclimatol. Palaeoecol.* **220**, 69–88 (2005).

83. P. D. Kruse, F. Debrenne, Ajax Mine archaeocyaths: A provisional biozonation for the upper Hawker Group (Cambrian stages 3-4), Flinders Ranges South Australia. *Australasian Palaeontological Memoirs* **53**, 1–238 (2020).

84. P. D. Kruse, Cyanobacterial-archaeocyathan-radiocyathan bioherms in the Wirrealpa Limestone of South Australia. *Can. J. Earth Sci.* **28**, 601–615 (1991).

85. R. Wood, A. G. Liu, F. Bowyer, P. R. Wilby, F. S. Dunn, C. G. Kenchington, J. F. H. Cuthill, E. G. Mitchell, A. Penny, Integrated records of environmental change and evolution challenge the Cambrian Explosion. *Nat. Ecol. Evol.* **3**, 528–538 (2019).

86. B. U. Haq, S. R. Schutter, A chronology of Paleozoic sea-level changes. *Science* **322**, 64–68 (2008).

87. A. Y. Zhuravlev, R. A. Wood, F. T. Bowyer, Cambrian radiation speciation events driven by sea level and redoxcline changes on the Siberian Craton. *Sci. Adv.* **9**, eadh2558 (2023).

88. R. D. Müller, J. Cannon, X. Qin, R. J. Watson, M. Gurnis, S. Williams, T. Pfaffelmoser, M. Seton, S. H. J. Russell, S. Zahirovic, GPlates: Building a virtual Earth through deep time. *Geochem. Geophys. Geosyst.* **19**, 2243–2261 (2018).

89. A. R. A. Aitken, D. A. Young, F. Ferraccioli, P. G. Betts, J. S. Greenbaum, T. G. Richter, J. L. Roberts, D. D. Blankenship, M. J. Siegert, The subglacial geology of Wilkes Land, East Antarctica. *Geophys. Res. Lett.* **41**, 2390–2400 (2014).

90. C. R. Scotese, "PALEOMAP PaleoAtlas for GPlates and the PaleoData Plotter Program" (PALEOMAP Project, Tech. Rep. 56, 2016).

91. J. W. Goodge, C. A. Finn, Glimpses of East Antarctica: Aeromagnetic and satellite magnetic view from the central Transantarctic Mountains of East Antarctica. *J. Geophys. Res.* **115**, (2010).

92. S. C. Cox, B. Smith Lyttle, S. Elkind, C. Smith Siddoway, P. Morin, G. Capponi, T. Abu-Alam, M. Ballinger, L. Bamber, B. Kitchener, L. Lelli, J. Mawson, A. Millikin, N. Dal Seno, L. Whitburn, T. White, A. Burton-Johnson, L. Crispini, D. Elliot, S. Elvevold, J. Goodge, J. Halpin, J. Jacobs, A. P. Martin, E. Mikhalsky, F. Morgan, P. Scadden, J. Smellie, G. Wilson, A continent-wide detailed geological map dataset of Antarctica. *Sci. Data* **10**, 250 (2023).

93. J. M. Miller, D. Phillips, C. J. L. Wilson, L. J. Dugdale, Evolution of a reworked orogenic zone: the boundary between the Delamerian and Lachlan fold belts, southeastern Australia. *Aust. J. Earth Sci.* **52**, 921–940 (2005).

94. S. Rocchi, L. Bracciali, G. di Vincenzo, M. Gemelli, C. Ghezzo, Arc accretion to the early Paleozoic Antarctic margin of Gondwana in Victoria Land. *Gondw. Res.* **19**, 594–607 (2011).

95. A. J. Rowell, M. N. Rees, R. A. Cooper, B. R. Pratt, Early Paleozoic history of the central Transantarctic Mountains: evidence from the Holyoake Range, Antarctica. *N. Z. J. Geol. Geophys.* **31**, 397–404 (1988).